THE ARCTIC REGIONAL CLIMATE SYSTEM MODEL: CURRENT STATUS AND RECENT RESULTS

Richard I. Cullather*, Amanda H. Lynch*,†, Andrew G. Slater* and Mark C. Serreze*

*Cooperative Institute for Research in Environmental Sciences, University of Colorado at Boulder
†Program in Atmospheric and Oceanic Sciences, University of Colorado at Boulder

1. INTRODUCTION

Conceptual models of the global general circulation typically have not included a separate high latitude frontal zone. As noted by Serreze et al. (2000), the notion of a region of frequent mesoscale frontal activity in northern high latitudes emerging as distinct from frontal activity in middle latitudes can be traced back to the early work of Dzerdzeevskii (1945). Reed and Kunkel (1960) named it the “Arctic frontal zone” and identified it to be a summer phenomenon distinct from the polar front. Bryson (1966) postulated that it was a year-round feature which is responsible for the position of the northern treeline. The Arctic front has been proposed variously to arise from the differential heating between snow-free land and cold Arctic Ocean in summer (Dzerdzeevskii 1945); from the interactions between these coastal constrasts and orography (Reed and Kunkel 1960); and in a turnaround of Bryson’s (1966) reasoning, from contrasts in surface heating between the tundra and boreal forest (Hare and Ritchie 1972; Pielke and Vidale 1995).

Serreze et al. (2000) examined the expression of this frontal zone in the NCEP/NCAR reanalysis data over the period 1979-1998 using a thermal front parameter (TFP). This analysis revealed a maximum in frontal frequencies over eastern Eurasia and Alaska in summer. This feature was easily distinguished from the polar front, and corresponded to an upper tropospheric jet, a preferred area for cyclogenesis, and a maximum in summertime precipitation. The frontal zone showed an association with orography and coastal contrasts, but the role of the tundra/boreal forest boundary (ecotone) could not be diagnosed due to the low resolution of the analyses.

Summer measurements on the Seward Peninsula in Alaska (Chapin and Beringer, unpublished data) found that, on a daily basis, the difference between the forest and tundra is only 5 Wm^{-2}, which is considerably less than the 50 Wm^{-2} cited by Pielke and Vidale (1995). They used their estimated daily sensible heat contrast of 50 Wm^{-2} to show that this influence, if spread out over a distance of 500 km and distributed within the 1000 to 500 mb layer, would be sufficient to be classified as a synoptic front.

Chapin and Beringer’s results show that the daily contrast is an order of magnitude less than that proposed by Pielke and Vidale (1995) and that the observed daily contrast would not be sufficient to influence the positioning of the arctic front. Midday contrasts, however, are likely to have an influence on local mesoscale convection at this interface and could be an important feedback to precipitation. An increase in precipitation over the forest interface along with higher daytime heat fluxes is potentially important in the maintenance or extension of the northern treeline.

To identify the necessary and sufficient forcing required to simulate an Arctic frontal zone, the Arctic Regional Climate System Model (Lynch et al. 1995, 1999) is used to determine the relative roles of coastal contrasts, topography and the treeline.

Corresponding author’s address: Amanda H. Lynch, PAOS/CIRES, Campus Box 216, University of Colorado, Boulder CO 80309-0216 USA; Tel. +1 303 492-5847, Fax +1 303 492-1149,
e-mail: `manda@cires.colorado.edu`.

2. FRONTAL DIAGNOSIS

To objectively determine the occurrence of fronts in model simulations, a variety of thermally and dynamically-based diagnostic tools are examined (following McInnes et al. 1994). We investigate such measures of baroclinicity as the near surface potential temperature gradient $|\underset{\sim}{\nabla}\theta|$ or the low level thickness gradient $|\underset{\sim}{\nabla}(\Delta Z)|$ (Pielke and Vidale 1995), and a thermal front parameter (Serreze et al. 2000)

$$-\underset{\sim}{\nabla}|\underset{\sim}{\nabla}T_{850}|\cdot\underset{\sim}{n}$$

where T_{850} is the 850 hPa temperature and $\underset{\sim}{n}$ is a unit vector in the direction of the 850 hPa temperature gradient. This parameter is a maximum where the temperature gradient is increasing most rapidly in the direction of an existing gradient, and placement of the front is on the warm side of the baroclinic zone.

Dynamical measures include the vertical component of relative vorticity

$$\zeta = \frac{\partial v}{\partial x} - \frac{\partial u}{\partial y}$$

and measures of the vertical motion such as the vertical velocity in pressure coordinates:

$$\omega = -\sigma\left\langle\int_0^{\sigma}\underset{\sim}{\nabla}\cdot p_s\underset{\sim}{u}d\sigma + \underset{\sim}{u}\cdot\underset{\sim}{\nabla}p_s\right\rangle$$

and the rate of change of the temperature gradient forced by the geostrophic wind, most simply expressed in a coordinate system aligned locally with the isotherms:

$$\underset{\sim}{Q} = -\frac{R}{p}\left|\frac{\partial T}{\partial y}\right|\underset{\sim}{k}\times\frac{\partial\underset{\sim}{u}}{\partial x}$$

where the vertical levels are in σ coordinates, $\underset{\sim}{u} = (u, v)$ is the horizontal wind on σ levels and p_s is the surface pressure. Since convergence of $\underset{\sim}{Q}$ implies upward motion, this can be used in place of ω as a diagnostic tool in the objective identification of the Arctic front. Such measures of frontal location are not confounded by signals from coastal contrasts as thermal measures are. The most unambiguous method of defining the position of a front is the axis of the relative vorticity maximum, particularly if advective rather than frontogenetic motion of the Arctic front is occurring.

3. MODEL AND EXPERIMENT DESCRIPTION

In order to isolate the necessary and sufficient elements required to force the location of the Arctic front, a series of sensitivity tests (Table 1) was conducted using the Arctic Regional Climate System Model (ARCSyM), a limited area model that includes comprehensive treatments of the atmosphere, ocean, sea ice and the land surface. The atmospheric component model includes physical parameterizations of convection and resolvable moist processes (Lynch et al. 1995); shortwave (Briegleb 1992) and longwave (Mlawer et al. 1997) radiation; and boundary layer processes (Holtslag et al. 1990). ARCSyM is forced at the lateral boundaries using temperature, wind, moisture, surface pressure and height fields provided from ECMWF operational analyses, which are updated every 12 hours at every vertical level. The atmospheric component is coupled to the NCAR Land Surface Model (Bonan 1996; Lynch et al. 1999). The sea ice is constrained to conform to SSM/I derived ice area, with ice and lead temperature calculated using the Parkinson and Washington (1979) ice thermodynamics, with modifications following Schramm et al. (1997). The model is configured over Alaska on a polar stereographic projection with a horizontal resolution of 30 km and 23 σ levels in the vertical. Three month integrations were performed for the periods January-March and June-August 1995, following a spin up period.

Experiment	Configuration
Control	January-March and June-August 1995.
No ecotone	As for the control, but with all vegetation in the domain replaced by tundra, so that the treeline contrast is removed.
No mountains	As for the control, but with land a uniform elevation of 10 m.
Coastal contrast	As for the control, but with uniform vegetation cover and uniform elevation.

Table 1: ARCSyM Sensitvity Tests

4. RESULTS

At this stage, the objective frontal diagnosis tools have been developed and tested, and the control experiment, no ecotone experiment and no mountains experiment have been completed. Fig. 1 shows an example of frontal locations diagnosed by TFP and vorticity, and a calculation of the Q-vector for a particular summer time slice in the control experiment.Although the

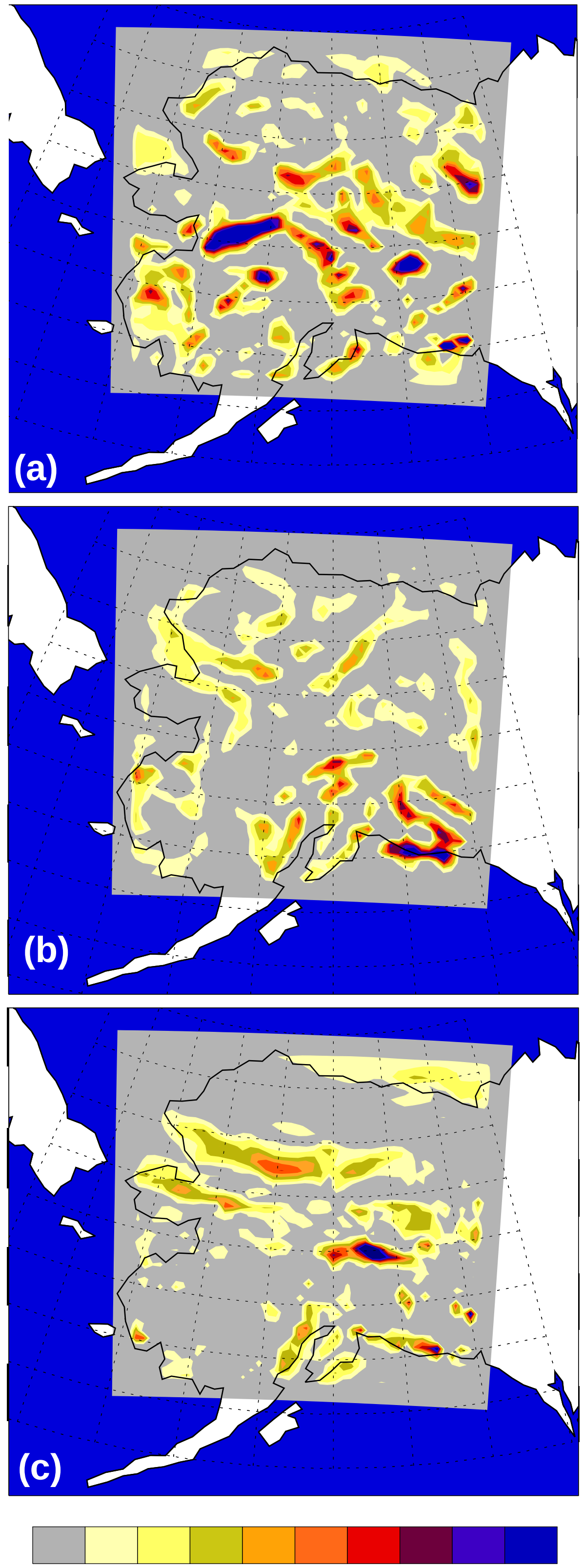

Figure 1. Control simulation valid at 12Z on the 22nd July 1995 as simulated in the control experiment. Shown for this date is (a) vorticity diagnostic calculated at the fifth σ level, with contour interval 2 s^{-1}; (b) TFP diagnostic calculated at the third σ level (0.8), and (c) Q-vector magnitude calculated at the fifth σ level (0.002 $m^2\ kg^{-1}\ s^{-1}$).

fields are quite noisy, activity associated with the Brooks Range and the Alaska Range appears to be important. Centers of action begin to emerge when a frequency analysis of these fields is performed on a longer experiment (not shown.)

A comparison of the control TFP diagnostic with this quantity for the no-ecotone and no-mountains experiments (Fig. 2). As can be seen, the no-ecotone case produces an almost identical response to the control case. However the no-mountains case shows a marked response, with minimal frontal activity on the particular day chosen. While these results are preliminary, they tend to support the suggestion by Serreze et al. (2000) that treeline forcing is not necessary to define frontal position.

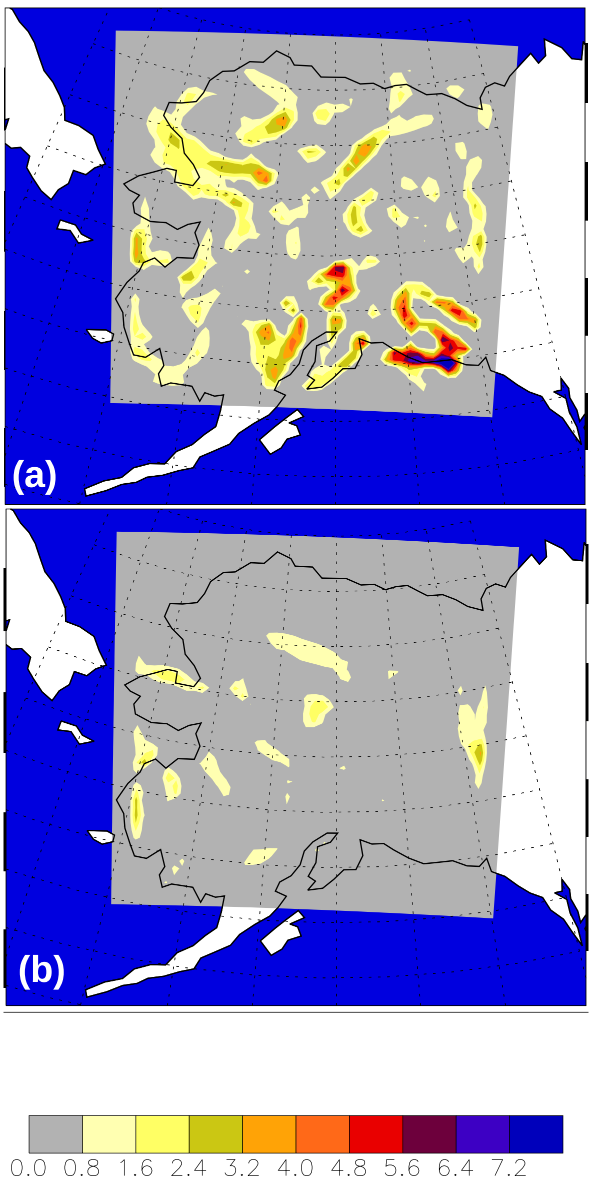

Figure 2. TFP diagnostic calculated at the third σ level valid 12Z, 22 July 1995, for (a) the no ecotone experiment and (b) no mountains experiment.

5. REFERENCES

Bonan, G.B., 1996: A land surface model (LSM version 1.0) for ecological, hydrological, and atmospheric studies: Technical description and user's guide. NCAR Tech Note NCAR/TN-417+STR, 165 pp.

Briegleb, B.P., 1992: Delta-Eddington approximation for solar radiation in the NCAR Community Climate Model. *J. Geophys. Res.*, **97**, 7603-7612.

Bryson, R.A., 1966: Air masses, stream lines and boreal forest. *Geogr. Bull.*, **8**, 228-269.

Dzerdzeevskii, B.L., 1945: Tsirkuliatsionnye skhemy v troposfere. Tsentral' noi Arktiki. *Izdatel' svo Akad. Nauk* [English transl. Sci. Rep. No. 3, Contract AF 19(122)-3228. UCLA].

Hare, F.K., and J.C. Ritchie, 1972: The boreal microclimates. *Geogr. Rev.*, **62**, 333-365.

Holtslag, A.A.M., E.I.F. de Bruijn, and H.L. Pan, 1990: A high resolution air mass transformation model for short-range weather forecasting. *Mon. Wea. Rev.*, **118**, 1561-1575.

Lynch, A.H., W.L. Chapman, J.E. Walsh, and G. Weller, 1995: Development of a regional climate model of the Western Arctic. *J. Climate*, **8**, 1555-1570.

Lynch, A.H., G.B. Bonan, F.S. Chapin III, and W.Wu, 1999: The impact of tundra ecosystems on the surface energy budget and climate of Alaska. *J. Geophys. Res.*, **104**, 6647-6660.

McInnes, K.L., J.J. BcBride, and L.M. Leslie, 1994: Cold fronts over southeastern Australia: Their representation in an operational numerical weather prediction model. *Wea. Forecasting*, **9**, 384-409.

Mlawer, E.J., S.J. Taubman, P.D. Brown, M.J. Iacono, and S.A. Clough, 1997: Radiative transfer for inhomogeneous atmospheres: RRTM, a validated correlated-k model for the longwave. *J. Geophys. Res.*, **102**, 16663-16682.

Parkinson, C.L., and W.M. Washington, 1979: A large-scale numerical model of sea-ice. *J. Geophys. Res.*, **84**, 311-337.

Pielke, R.A., and P.L. Vidale, 1995: The boreal forest and the polar front. *J. Geophys. Res.*, **100**, 25755-25758.

Reed, R.J., and B.A. Kunkel, 1960: The Arctic circulation in summer. *J. Meteor.*, **17**, 489-506.

Schramm, J.L., M.M. Holland, J.A. Curry, and E.E. Ebert, 1997: Modeling the thermodynamics of a sea ice thickness distribution. Part 1: Sensitivity to ice thickness resolution. *J. Geophys. Res.*, **102**, 23079-23091.

Serreze, M.C., A.H. Lynch, and M.P. Clark, 2000: The summer Arctic frontal zone. *J. Climate* (in review).